Journal of Solid State Chemistry 182 (2009) 913–919

Contents lists available at ScienceDirect

Journal of Solid State Chemistry

journal homepage: www.elsevier.com/locate/jssc

Syntheses, crystal structures, and characterization of As(III) and As(V) thioarsenates, $[Mn_2(phen)(As^{III}_2S_5)]_n$ and $[Mn_3(phen)_3(As^{V}S_4)_2]_n \cdot nH_2O$

Xin Wang [a,b], Tian-Lu Sheng [a], Sheng-Min Hu [a], Rui-Biao Fu [a], Jian-Shan Chen [a], Xin-Tao Wu [a,*]

[a] State Key Laboratory of Structural Chemistry, Fujian Institute of Research on the Structure of Matter, Chinese Academy of Sciences, Fuzhou, Fujian 350002, PR China
[b] Graduate University of Chinese Academy of Sciences, Beijing 100039, PR China

ARTICLE INFO

Article history:
Received 27 November 2008
Received in revised form
13 January 2009
Accepted 18 January 2009
Available online 5 February 2009

Keywords:
Manganese
Thioarsenate(III)
Multiple physical properties
Thermoanalysis
Semiconductor
Magnetism

ABSTRACT

The hydrothermal reactions of As, Mn, S, phen (phen = 1,10-phenanthroline), and en (en = ethylenediamine) yield two manganese As(III) and As(V) thioarsenates, $[Mn_2(phen)(As^{III}_2S_5)]_n$ (**1**) and $[Mn_3(phen)_3(As^{V}S_4)_2]_n \cdot nH_2O$ (**2**), respectively. Single-crystal X-ray diffraction analyses reveal that compound **1** is a two-dimensional (2D) layer of (6,3) topology. The 18-membered rings within the 2D porous layers are formed by corner-, edge-, and face-sharing cubane-like $[Mn_2As_2S_4]$ units along the [100] direction. Whereas compound **2** is a one-dimensional (1D) chain structure. They are both characterized by IR, elemental analysis, EDS, and X-ray powder diffraction. The thermogravimetric analysis of **1** and **2** are discussed. Both the compounds are semiconductors with the band gap of E_g (compound **1**) = 2.01 eV (617 nm) and E_g (compound **2**) = 1.97 eV (629 nm), respectively. In addition, the variable-temperature magnetic susceptibility data suggest weak antiferromagnetic interactions between the Mn^{2+} ions in these two compounds.

1. Introduction

There is currently a great deal of interest in the synthesis, structures, and properties of new chalcogenide-based materials due to their potential applications, for example in optoelectronic materials, molecule-discriminating catalysis, ion-exchangers, nonlinear optical (NLO) materials, chemical sensing applications, and semiconductors [1–5]. Particularly, crystalline chalcogenides exemplified by a large number of quaternary/ternary $M/E'/E$ clusters and open frameworks (M = transition metal, E' = heavy group 13–15 element, E = S, Se, Te) with intriguing applications, ranging from semiconductors to gas separation, have received increasing attention at present [6–7]. During the past two decades, we have focused on the synthetic and structural chemistry of the transition metal/main group element-sulfur compounds [8–10], such as molybdenum(tungsten)/copper (silver) thiolates, tin sulfide (oxosulfide) compounds, thioantimonates [11–14]. Now we further spread our interest to the study of thioarsenates.

At present, there are numerous examples of thioarsenates(III) with higher nuclearity $[As^{III}_xS_y]^{n-}$ units synthesized by molten salt (flux), hydrothermal or solvothermal methods [15,16]. One of the most effective and attractive principle established by the exploration of thioarsenates(III) is the self-condensation of the fundamental building unit $[As^{III}S_3]^{3-}$, which undergoes various types of condensation reactions, ranging from oligomeric chain to ring formation. In this way, dozens of thioarsenates(III) with novel anionic building units from isolated building blocks to infinite frameworks have been synthesized [17–21]. Usually, the type and identity of the $[As^{III}_xS_y]^{n-}$ anions lie on the suitable charge-matching of templating agents, such as transition-metal compounds cations or organic amine cations species. Compared with overwhelming thioarsenates(III), however, only a few thioarsenates(V) have been published to date. Unlike $[As^{III}S_3]^{3-}$, the $[As^{V}S_4]^{3-}$ anions are seldom interconnected to form poly-anions, and they usually present as the isolated tetrahedral structural motif except that in some case $[As^{V}S_4]^{3-}$ anions are bound to the metal centers, examples are $[As^{V}S_4]^{3-}$ anions as ligands coordinating to the transition metal centers in chains $[Mn(dien)AsS_4^-]_\infty$ (dien = diethyleneamine) and $[AgAsS_4^{2-}]_\infty$ [22–24], or coordinating to lanthanide metal centers in $K_3Ln(AsS_4)_2$ (Ln = Nd, Sm, Gd) [25].

Particularly, new functional materials of thioarsenates with multiple physical properties have attracted much attention [26,27]. The incorporation of the optical, magnetic, and electronic properties of transition-metal compounds into the main group network can help to introduce complementary properties and synergistic effects [28]. Moreover, the existence of in situ generated $[M(N\text{-donor})_m]^{n+}$ under hydro- or solvothermal conditions is highly desirable in terms of magnetic, conductive and luminescent behavior [29], which has been proven to be an excellent structure-directing reagent in the metal-chalcogenide

* Corresponding author. Fax: +86 591 8371 4946.
E-mail address: wxt@fjirsm.ac.cn (X.-T. Wu).

0022-4596/$ - see front matter © 2009 Elsevier Inc. All rights reserved.
doi:10.1016/j.jssc.2009.01.021

system. Herein, we report the hydrothermal preparation of two new thioarsenates $[Mn_2(phen)(As_2^{III}S_5)]_n$ **(1)** and $[Mn_3(phen)_3(As^{V}S_4)_2]_n \cdot nH_2O$ **(2)** (phen = 1,10-phenanthroline).

2. Experimental section

2.1. Materials

The reagents arsenic powder (As, 70 mesh, 99.99%), sulfur powder (S, 99.5%), manganese powder (Mn, 325 mesh, 99.99%), 1,10-phenanthroline (phen), and ethylenediamine (en) were commercial available (from Acros, Fluka, Alfa Aesar or Sinopharm Chemical Reagent Co., Ltd.). All of the chemicals were obtained from commercial sources without further purification.

2.2. Physical measurements

Elemental analyses were performed with a Vario EL III Etro Elemental Analyzer. Semiquantitative Microprobe Analysis was performed using a FE-SEM (JSM6700F) equipped with an energy dispersive spectroscopy (EDS) detector. Powder X-ray diffraction (XRD) patterns were acquired on a DMAX-2500 diffractometer using Cu$K\alpha$ radiation in the ambient environment. Infrared spectra were recorded on a Nicolet magna 750 FT-IR spectrophotometer using KBr pellets in the range of 400–4000 cm^{-1}. The diffuse reflectance spectra were recorded on a PerkinElmer Lambda 35 UV–vis spectrometer, $BaSO_4$ powder was used as a reference (100% reflectance) and base material, on which the ground powder samples were coated. Magnetic measurements for the two compounds were carried out with a Quantum Design PPMS model 6000 magnetometer at 1 KOe in the temperature range of 2–300 K. Thermogravimetric analysis (TGA) was performed on a computer controlled NETZSCH STA449C under a steady flow under dry nitrogen gas at a heating rate of 10 °C/min (Al_2O_3 crucible was used as a reference).

2.3. X-ray crystallography

Single crystals suitable for X-ray diffraction, with dimensions of $0.16 \times 0.12 \times 0.03$ mm for **1**, and $0.16 \times 0.18 \times 0.20$ mm for **2**, were mounted on the top of a glass fiber. Diffraction data for compound **1** were measured on a Siemens SMART-CCD diffractometer equipped with a graphite-monochromatic Mo$K\alpha$ radiation ($\lambda = 0.71073$ Å) at 293(2) K, while data for compound **2** were measured on a Rigaku Mercury CCD diffractometer with Mo$K\alpha$ radiation ($\lambda = 0.71073$ Å) at 293(2) K. Data were reduced with *CrystalClear* version 1.3. The structure was solved by direct methods. All non-hydrogen atoms were located by direct methods and refined by full-matrix least-squares techniques on F^2 using *SHELXTL-97* version 5 package of crystallographic software [30,31]. The H atoms bound to C were located by geometrical calculations, and their positions and thermal parameters were fixed during the structure refinement. We have tried to located the H atoms of isolated water molecules in compound **2** but not found them. The crystallographic data collection and structural refinements for the two compounds are summarized in Table 1. Selected bond lengths (Å) and bond angles (°) for compounds **1** and **2** are listed in Tables 2 and 3, respectively.

2.4. Synthesis of $[Mn_2(phen)(As_2^{III}S_5)]_n$ (1)

A mixture of As (74.9 mg, 1 mmol), Mn (54.9 mg, 1 mmol), S (96.2 mg, 3 mmol), phen (78 mg, 0.5 mmol), en (0.2 ml, 3 mmol), and distilled water (5 mL, 278 mmol) was sealed in a 25 mL poly(tetrafluoroethylene)-lined stainless steel container under autogenous pressure and then heated at 423 K for 5 days under autogenous pressure. After the mixture was subsequently allowed to cool slowly to ambient temperature, prism shaped orange crystals were obtained. The crystals were filtered, washed with ether and ethanol, and dried at ambient temperature. The EDS for **1** show the mean mole ratio of Mn^{2+} ions to As^{3+} ions is 1.06, in agreement with the ratio value of 1 from the formula (Fig. S1). The experimental patterns are in good agreement with the

Table 1
Crystal data collection and structural refinement parameters for **1** and **2**.

Compound	**1**	**2**
Formula	$C_{12}H_8As_2Mn_2N_2S_5$	$C_{36}H_{26}As_2Mn_3N_6OS_8$
Fw	600.22	1129.77
a (Å)	12.494(9)	15.191(3)
b (Å)	12.254(8)	13.450(3)
c (Å)	12.352(9)	20.991(5)
β (deg)	112.034(12)	90.00
V (Å^3)	1753(2)	4288.6(16)
Z	4	4
Crystal system	Monoclinic	Orthorhombic
Space group	$P2_1/c$	*Pbcn*
p (g/cm^3)	2.274	1.750
μ (mm^{-1})	5.778	2.829
Total reflections	12 696	31 420
Independent reflections	3875	4918
R_{int}	0.0420	0.0343
Observed reflections ($I > 2\sigma(I)$)	2679	4345
Parameters refined	208	243
*R*1, *wR*2 ($I > 2\sigma(I)$)	0.0354, 0.0649	0.0527, 0.1311
*R*1, *wR*2 (all data)	0.0612, 0.0763	0.0598, 0.1368
GOF	1.047	1.105

$R = \sum(||F_o|-|F_c||)/\sum|F_o|$, $wR2 = \{\sum w[(F_o^2-F_c^2)]^2/\sum w[(F_o^2)^2]\}^{1/2}$, $w = 1/[\sigma^2(F_o^2)+(aP)^2+bP]$, $P = (F_o^2+2F_c^2)/3]$. For **1**, $a = 0.0283$ and $b = 0.3287$; for **2**, $a = 0.0641$ and $b = 8.4441$.

Table 2
Selected bond lengths (Å) and bond angles (°) for compound **1**.

Bond	(Å)	Bond	(Å)
As(1)–S(3)	2.2321(15)	As(2)–S(4)	2.2534(14)
As(1)–S(2)	2.2440(16)	As(2)–S(5)	2.2674(17)
As(1)–S(1)	2.3492(14)	As(2)–S(1A)	2.3359(14)
Mn(1)–N(1)	2.247(3)	Mn(2)–S(4)	2.5395(18)
Mn(1)–N(2)	2.257(3)	Mn(2)–S(3)	2.6024(16)
Mn(1)–S(3)	2.5492(18)	Mn(2)–S(2B)	2.6102(17)
Mn(1)–S(2)	2.5542(16)	Mn(2)–S(5)	2.6438(16)
Mn(1)–S(4)	2.6539(17)	Mn(2)–S(5C)	2.6461(16)
Mn(2)–S(1B)	2.6926(18)	Mn(1)–S(5B)	2.9305(18)
Angle	**(°)**	**Angle**	**(°)**
S(3)–As(1)–S(2)	100.29(6)	S(4)–As(2)–S(5)	99.40(5)
S(3)–As(1)–S(1)	100.43(6)	S(4)–As(2)–S(1A)	97.14(6)
S(2)–As(1)–S(1)	97.86(6)	S(5)–As(2)–S(1A)	95.58(5)
N(1)–Mn(1)–N(2)	74.34(13)	N(1)–Mn(1)–S(4)	93.10(9)
N(1)–Mn(1)–S(3)	107.07(10)	N(2)–Mn(1)–S(4)	87.67(10)
N(2)–Mn(1)–S(3)	176.04(9)	N(2)–Mn(1)–S(2)	94.66(10)
N(1)–Mn(1)–S(2)	164.41(9)	S(4)–Mn(2)–S(5C)	94.04(6)
S(3)–Mn(1)–S(2)	84.64(6)	S(3)–Mn(2)–S(5C)	173.69(4)
S(3)–Mn(1)–S(4)	88.55(5)	S(2B)–Mn(2)–S(5C)	90.39(6)
S(2)–Mn(1)–S(4)	97.53(6)	S(5)–Mn(2)–S(5C)	93.21(6)
S(4)–Mn(2)–S(3)	89.91(5)	S(4)–Mn(2)–S(1B)	173.43(4)
S(4)–Mn(2)–S(2B)	98.47(5)	S(3)–Mn(2)–S(1B)	96.62(6)
S(3)–Mn(2)–S(2B)	84.15(6)	S(2B)–Mn(2)–S(1B)	81.54(5)
S(4)–Mn(2)–S(5)	83.37(5)	S(5)–Mn(2)–S(1)	97.06(5)
S(3)–Mn(2)–S(5)	92.13(6)	S(5C)–Mn(2)–S(1B)	79.39(6)
S(2B)–Mn(2)–S(5)	175.83(4)		

Symmetry codes for **1**: A: $-x, y-1/2, -z+1/2$; B: $x, -y-1/2, z-1/2$; C: $-x, -y-1, -z$.

theoretical ones generated from the single-crystal X-ray data of the compound **1**, clearly indicating the good purity of the compound (Fig. S3). The yield: 38% (114.0 mg, based on As). *Anal. Calc.* for **1** $C_{12}H_8As_2Mn_2N_2S_5$ (600.22): H 1.34, C 24.01, N 4.67; Found: H 1.39, C 23.82, N 4.44. IR spectra (KBr, cm^{-1}): 3458(w) (ν_{O-H}), 3040(s) (ν_{Ar-H}), 1603(w), 1599(s), 1580(s), 1500(s) ($\nu_{Ar-C=C}$), 1480(s), 1450(s), 1417(m), 1321(m), 1211(w), 1144(w), 1103(w), 995(m), 850(s), 771(m), 721(w) (Fig. S5).

2.5. Synthesis of $[Mn_3(phen)_3(As^VS_4)_2]_n \cdot nH_2O$ (**2**)

A mixture of As (74.9 mg, 1 mmol), Mn (54.9 mg, 1 mmol), S (224.4 mg, 7 mmol), phen (78 mg, 0.5 mmol), en (0.2 ml, 3 mmol), and distilled water (5 mL, 278 mmol) was sealed in a 25 mL poly(tetrafluoroethylene)-lined stainless steel container under autogenous pressure and then heated at 423 K for 5 days under autogenous pressure. After the mixture was subsequently allowed to cool slowly to ambient temperature, prism shaped orange crystals were obtained. The crystals were filtered, washed with ether and ethanol, and dried at ambient temperature. The EDS for **2** show the mean mole ratio of Mn^{2+} ions to As^{5+} ions is 1.57, in agreement with the ratio value of 1.5 from the formula (Fig. S2). The experimental patterns are in good agreement with the theoretical ones generated from the single-crystal X-ray data of the compound **2**, clearly indicating the good purity of the compound (Fig. S4). The yield: 23% (130.1 mg, based on As). *Anal. Calc.* for **2** $C_{36}H_{26}As_2Mn_3N_6OS_8$ (1129.77): H 2.32, C 38.27, N 7.44; found: H 2.38, C 38.49, N 7.26. IR spectra (KBr, cm^{-1}): 3510(m) (ν_{O-H}), 3048(w) (ν_{Ar-H}), 1630(m), 1600(w), 1580(m), 1506(m), 1452(w) ($\nu_{Ar-C=C}$), 1419(s), 1337(w), 1216(w), 1138(m), 1096(m), 886(m), 846(s), 772(w), 730(s), 644(s) (Fig. S6).

Table 3
Selected bond lengths (Å) and bond angles (º) for compound **2**.

Bond	(Å)	Bond	(Å)
As(1)–S(3)	2.1303(13)	As(1)–S(2)	2.1726(11)
As(1)–S(4)	2.1379(14)	As(1)–S(1)	2.1800(11)
Mn(1)–N(2)	2.252(3)	Mn(2)–N(3)	2.279(5)
Mn(1)–N(1)	2.255(3)	Mn(1)–S(1)	2.6511(12)
Mn(1)–S(2)	2.5941(13)	Mn(2)–S(3)	2.5588(15)
Mn(1)–S(4A)	2.6315(15)	Mn(2)–S(2)	2.6754(11)
Mn(1)–S(1A)	2.6457(12)		
Angle	**(°)**	**Angle**	**(°)**
S(3)–As(1)–S(4)	115.56(6)	S(3)–As(1)–S(1)	113.58(6)
S(3)–As(1)–S(2)	105.14(5)	S(4)–As(1)–S(1)	103.77(5)
S(4)–As(1)–S(2)	112.90(5)	S(2)–As(1)–S(1)	105.65(4)
N(1)–Mn(1)–S(1)	93.42(10)	N(1)–Mn(1)–S(1A)	167.69(10)
N(1)–Mn(1)–S(2)	104.46(10)	N(1)–Mn(1)–S(4A)	87.63(10)
N(2)–Mn(1)–S(1A)	107.35(9)	N(2)–Mn(1)–S(4A)	88.90(10)
N(2)–Mn(1)–S(2)	90.93(10)	N(2)–Mn(1)–N(1)	73.62(13)
S(2)–Mn(1)–S(4A)	167.34(5)	N(3B)–Mn(2)–N(3)	76.3(4)
S(2)–Mn(1)–S(1A)	87.84(4)	N(3)–Mn(2)–S(3)	95.7(2)
S(4A)–Mn(1)–S(1A)	80.15(4)	N(3)–Mn(2)–S(3B)	155.49(14)
N(2)–Mn(1)–S(1)	163.78(10)	S(3)–Mn(2)–S(3B)	100.19(9)
S(2)–Mn(1)–S(1)	82.78(4)	N(3)–Mn(2)–S(2B)	79.32(14)
S(4A)–Mn(1)–S(1)	100.49(4)	N(3)–Mn(2)–S(2)	108.53(13)
S(1A)–Mn(1)–S(1)	87.41(4)	S(3)–Mn(2)–S(2)	81.48(4)
S(2B)–Mn(2)–S(2)	170.34(6)	S(3)–Mn(2)–S(2B)	92.30(4)

Symmetry codes for **2**: A: $-x, -y+1, -z$; B: $-x, y, -z+1/2$.

3. Results and discussion

3.1. Syntheses

Syntheses of the compounds are shown in Scheme 1. Typically, As, Mn, S, phen, and en were stirred homogeneously and sealed in 25 mL of poly(tetrafluoroethylene)-lined stainless steel vessels at 423 K for 5 days, yielding the products. It was found, however, that the oxidation-state of As in the thioarsenates polymers were associated with the molar ratio of S to As. Compound $[Mn_2(phen)(As^{III}_2S_5)]_n$ (**1**; 38% yield) was produced when the molar ratio of S to As was 3:1, whereas $[Mn_3(phen)_3(As^VS_4)_2]_n \cdot nH_2O$ (**2**; 23% yield) was generated when the molar ratio of S to As was 7:1. It has been reported that antimony/arsenic with different value is related to the molar ratio of the reactants [32]. In the presence of en, the excess amount of elemental S would be beneficial to the oxidization of $E'^{III}S_3^{3-}$ to $E'^{V}S_4^{3-}$. This can also be supported by the fact that when the S/As molar ratio is less than 3, the thioarsenates(III) are generated, such as $[M(en)_3]_2As_2S_5$ (M = Mn, Ni) (S/As = 1.5) [33], $(Ph_4P)_2[Hg_2As_4S_9]$ (S/As = 3) [34], $(Ph_4P)_2[Pt(As_3S_5)_2]$ (S/As = 3) [35], $[K(2.2.2\text{-cryptand})]_2[As_2S_4] \cdot 2CH_3CN$ (S/As = 1) [36]. On the other hand, when the S/As molar ratio is greater than 3, the thioarsenates(V) are produced, such as $[Co(C_2H_8N_2)_3]AsS_4$ (S/As = 3.5) [37].

To investigate the effect of en to the final product, a series of parallel reactions have been done. The experimental results showed that by the same starting materials and under the same hydrothermal conditions, different products would be obtained with different amount of en. When en was less than 1 mL, compounds **1** (S/As = 3) and **2** (or S/As = 7) were generated, respectively. When en was more than 1 mL, unknown pulverous residues were found. When the reaction was carried out in the absence of en, $[(phen)MnCl_2]_n$ was produced, suggesting that a small quantity of en is necessary for the formation of the thioarsenates.

3.2. Description of crystal structures

3.2.1. $[Mn_2(phen)(As^{III}_2S_5)]_n$ (**1**)

Single-crystal X-ray diffraction reveals that compound **1** crystallizes in the monoclinic space group $P2_1/c$ and gives a two-dimensional (2D) layer of (6,3) topology (Fig. S7). As shown in Fig. 1, the As^{III} atom locates in a trigonal pyramid coordination

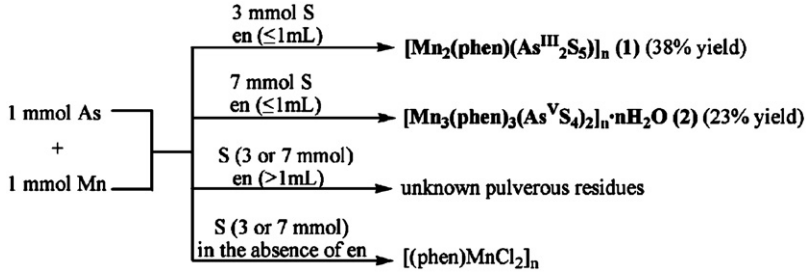

Scheme 1. The reaction route with different reaction conditions (water is 5 mL).

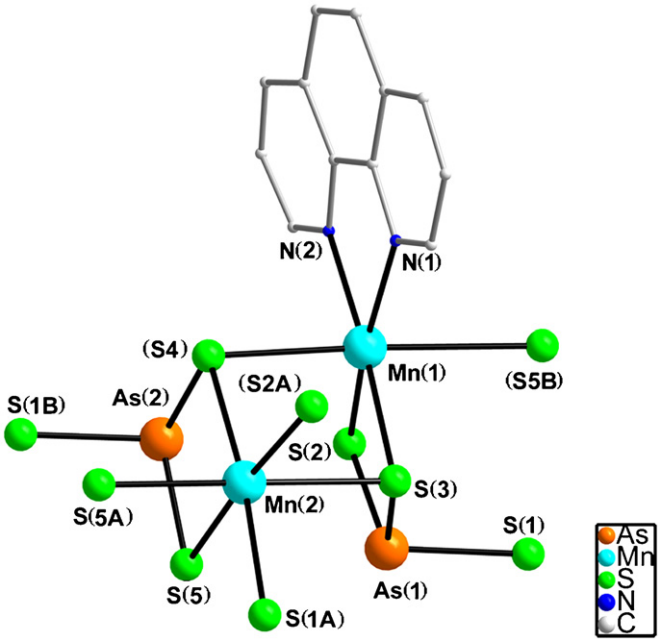

Fig. 1. Ball–stick representations show the coordination environment of Mn and As in **1**. Symmetry code: A: $-x, y-1/2, -z+1/2$; B: $x, -y-1/2, z-1/2$.

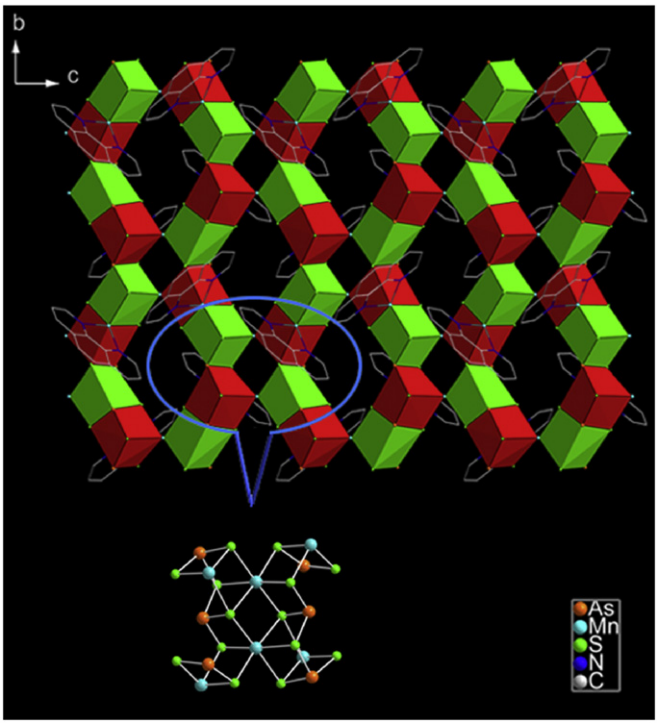

Fig. 2. Polyhedral view of 2D layer showing the cubane-like arrangements in compound **1** along the *a*-axis. Hydrogen atoms are omitted for clarity.

environment with three S atoms, and the As–S bond distances range from 2.2321(15) (As(1)–S(3)) to 2.3492(14) (As(1)–S(1)) Å, which are the typical distances of As–S found in other compounds containing $[As^{III}S_3]^{3-}$ anions [27]. There are two distinct coordination modes for the two independent Mn atoms, the Mn(1) atom is in a severely distorted $[MnN_2S_4]$ octahedral coordination environment with two N donors from one phen and four S atoms. The distances of Mn–N and Mn–S are in the ranges 2.247(3) (Mn(1)–N(1)) to 2.257(3) (Mn(1)–N(2)) Å and 2.5492(18) (Mn(1)–S(3)) to 2.9305(18) (Mn(1)–S(5B)) Å, respectively, similar to those found in other $Mn_2(L)As_2S_5$ and $Mn_2(L)Sb_2S_5$ containing Mn–N and Mn–S bonds [38,39]. The remarkably long Mn(1)–S(5B) bond may be caused by the steric constraints of phen ligands [24]. The Mn(2) atom is in a slightly distorted $[MnS_6]$ octahedral coordination geometry, which is surrounded by six S atoms. The Mn–S distances from 2.5395(18) (Mn(2)–S(4)) to 2.6926(18) (Mn(2)–S(1B)) Å, are comparable to those reported [27,39]. The trigonal pyramidal $[AsS_3]$ units, $[MnN_2S_4]$ and $[MnS_6]$ octahedra are linked together to yield cubane-like $[Mn_2As_2S_4]$ units. The 18-membered rings within the 2D porous layers are formed by corner-, edge-, and face-sharing cubane-like $[Mn_2As_2S_4]$ units on the [100] plane (Fig. 2), with the Mn···Mn distances of 3.634 (Mn2···Mn2D), 3.678 (Mn1···Mn2), 3.837 (Mn1C···Mn2) Å, respectively. Furthermore, the weak π–π stacking interactions of pyridyl rings of phens (distance: 3.596 Å) between the adjacent 2D layers stabilize the final three-dimensional (3D) supermolecular structure (Figs. S8–10).

3.2.2. $[Mn_3(phen)_3(As^VS_4)_2]_n \cdot nH_2O$ (**2**)

Single-crystal X-ray diffraction reveals that compound **2** crystallizes in the orthorhombic space group *Pbcn* consisting of 1D chains and guest water molecules. As shown in Fig. 3, the asymmetric unit of **2** contains one As(III) atom, one and a half Mn(II) atoms, one and a half phen ligands, four S atoms and a half lattice water. The As^V atom is four-coordinated by four S atoms in a tetrahedral geometry. There are two kinds of bridging coordination modes of the S atoms, μ_2-S and μ_3-S, with As–S distances from 2.1303(13) Å (As(1)–S(3)) to 2.1800(11) Å (As(1)–S(1)), which are slightly shorter than As–S distances in literature [21,40]. The Mn atom locates in a $[MnN_2S_4]$ distorted-octahedral coordination geometry, in which the Mn atom is joined by two nitrogen atoms from one phen and four S atoms from two AsS_4 tetrahedra. The equatorial plane is defined by two nitrogen atoms of a chelating phen group and two μ_3-S atoms from two different $[AsS_4]^{3-}$ anions. Another two μ_2-S atoms from the AsS_4 units occupy the axial positions of the octahedron. The Mn–N bond lengths range from 2.252 Å (Mn(1)–N(2)) to 2.279(5) Å (Mn(2)–N(3)) and the Mn–S bond lengths range from 2.5588(15) Å (Mn(2)–S(3)) to 2.6754(11) Å (Mn(2)–S(2)), which are all within the normal ranges [21,22]. Two neighboring $[MnN_2S_4]$ octahedra are edge-shared by two equatorial direction S atoms to form a $[Mn_2]$ unit with Mn···Mn distance of 3.829 Å (Fig. 4). The $[Mn_2]$ units together with two neighboring $[AsS_4]$ pyramids are edge-shared further to form a $[Mn_2As_2]$ unit. And finally these $[Mn_2As_2]$ units are linked by another $[MnN_2S_4]$ octahedron to form one-dimensional (1D) chains running along the [001] direction (Mn(1)···Mn(2)): 4.671 Å; Mn(1A)···Mn(2): 4.443 Å). In addition, the lattice water molecules are sandwiched by the phen ligands (Fig. S11).

3.3. Thermogravimetric analyses

Thermal behaviors of **1** and **2** were investigated using TGA–differential thermal analysis (DTA). As shown in Fig. 5, there was only one sharp weight loss of 29.8% occurred in compound **1**, which was accompanied by the endothermic event at $T_e = 322$ °C and $T_p = 344$ °C in the DTA curve. The experimental value is in good agreement with that determined for the removal of the one phen ligand ($-\Delta_{m,theo} = 30.2\%$). The mechanism of decomposition for compound **2** is more complicated and three obvious steps can be identified (Fig. 6). In the first step, the TGA curve exhibits a mild weight-loss step from 102 °C up to 291 °C, with the observed weight loss of 1.7% corresponding to the release of water

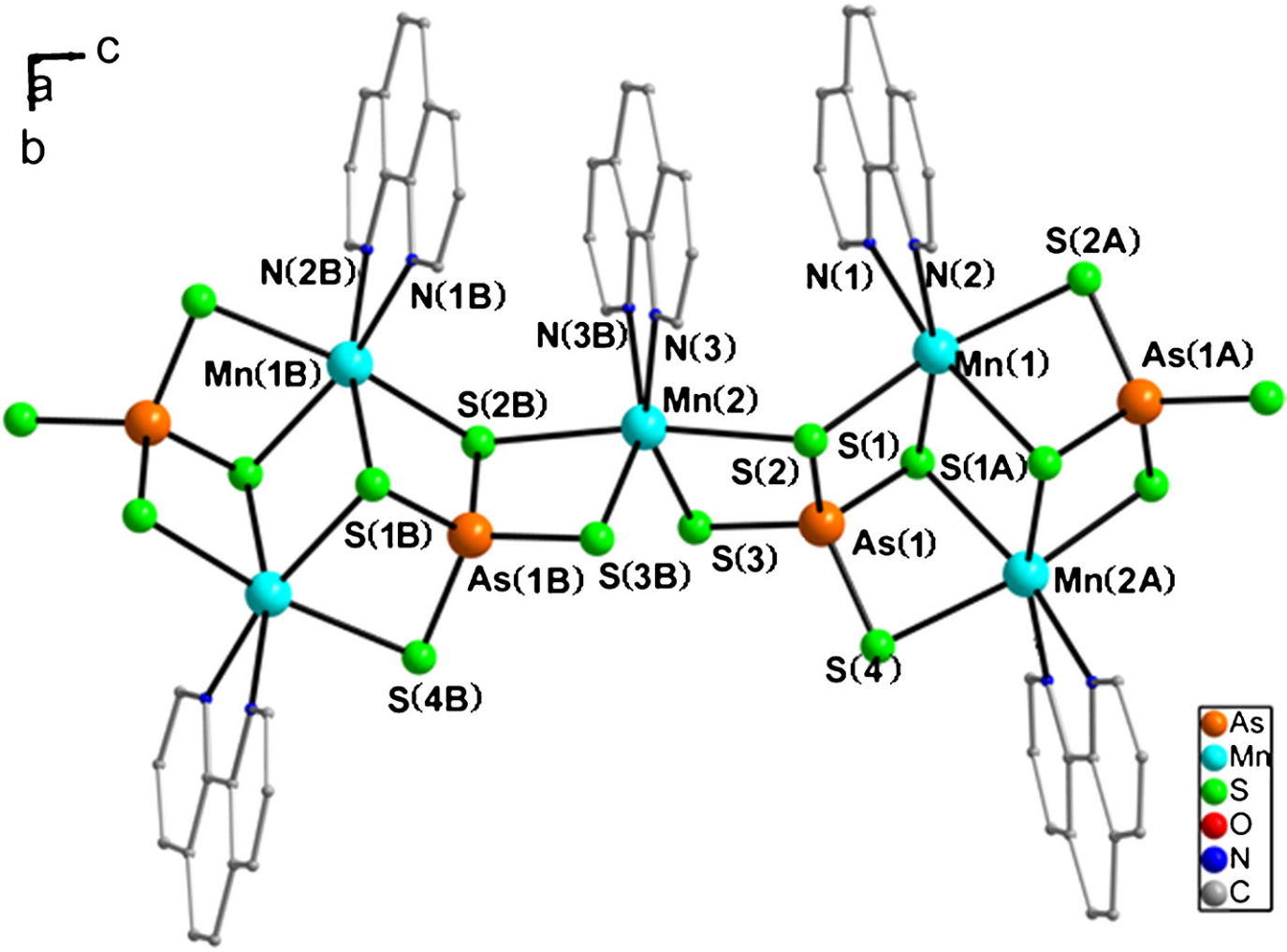

Fig. 3. Ball–stick representations show the coordination environment in **2**. Symmetry codes: A: $-x,-y+1,-z$; B: $-x,y,-z+1/2$.

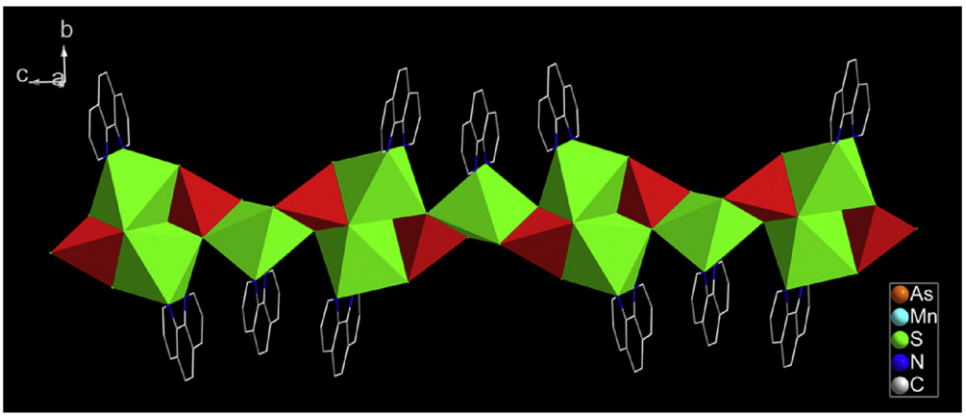

Fig. 4. Polyhedral view of the 1D chain along the [010] direction in compound **2**. Green octahedron: [MnN_4S_2]; red tetrahedron: [AsS_4]. Hydrogen atoms are omitted for clarity. (For interpretation of the reference to color in this figure legend, the reader is referred to the web version of this article.)

molecules (Calcd. 1.6%). On further heating, another endothermic event occurred with the DTA signal at $T_p = 370\,^{\circ}C$, following that, there is the third weight loss up to 600 °C, the total mass loss of the last two steps is 31.1% which can be attributed to the removal of three phen ligands ($-\Delta_{m,theo} = 31.9\%$).

3.4. Magnetic properties

The variable-temperature magnetic susceptibility data for compounds **1** and **2** were collected for the pure crystal samples under 1 KOe external field in the temperature range 2–300 K. The crystals'

purities were confirmed by PXRD. The magnetic properties for **1** and **2** in the form of χ_m vs. T, $1/\chi_m$ vs. T and μ_{eff} vs. T plots are shown in Figs. 7. and 8, respectively. The μ_{eff} value at 300 K is equal to $5.21\mu_B$ and $5.33\mu_B$ for **1** and **2**, respectively, which is slightly lower than the expected value of $5.92\mu_B$ for per Mn(II) ion. Upon cooling, the μ_{eff} value decreases continuously to $0.88\mu_B$ and $1.00\mu_B$ at 2 K for **1** and **2**, respectively, suggesting a dominant antiferromagnetic interaction between Mn(II) ions in these two compounds. A Curie Weiss fit to the 100–300 K susceptibility data yields $C = 5.00\,\text{emu K mol}^{-1}$, $\theta = -134.84$ K for **1**, and $C = 3.56\,\text{emu K mol}^{-1}$, $\theta = -62.74$ K for **2**, also indicating the antiferromagnetic coupling between Mn(II) ions. Furthermore, the χ_m value for **1** and **2** increases gradually to a maximum and decreases on further cooling finally with Néel temperatures of 26 and 16 K, respectively, confirming the antiferromagnetic interactions. Furthermore, the antiferromagnetic nature of the complex is supported by the magnetization (M) vs field (H) curve measured at 2 K (Fig. S12 and Fig. S13). The M–H curve shows a nearly linear increase with increasing field, and then the magnetization increases gradually to 90 KOe without saturation for two compounds.

3.5. Optical diffuse reflectance measurements

The optical diffuse reflectance measurements were carried out at room temperature. The absorption data were calculated using the Kubelka–Munk function $\alpha/S = (1-R)^2/2R$ [41], where R is the reflectance at a given energy, α the absorption and S the scattering coefficient. The band gap energy value was determined by extrapolation from the linear portion of the absorption edge in (α/S) versus energy plot. As the absorption spectra of **1** and **2** shown in Fig. S14 and Fig. S15, the obtained absorption versus energy spectra show band gaps at 2.01 eV (617 nm) for **1**, and 1.97 eV (629 nm) for **2**, respectively, which are in agreement with the color of the crystals and suggest the two compounds are semiconductors. All of these values are in the typical range reported in other thioarsenates [24].

4. Conclusions

In summary, hydrothermal syntheses, single-crystal structures, characterization (including IR, elemental analysis, EDS, XRD, UV–vis, and DTA-TG measurements) and magnetic properties of the two semiconductors, manganese As(III) and As(V) thioarsenates have been described. The same starting reactants with different molar ratio result in two different oxidation-state

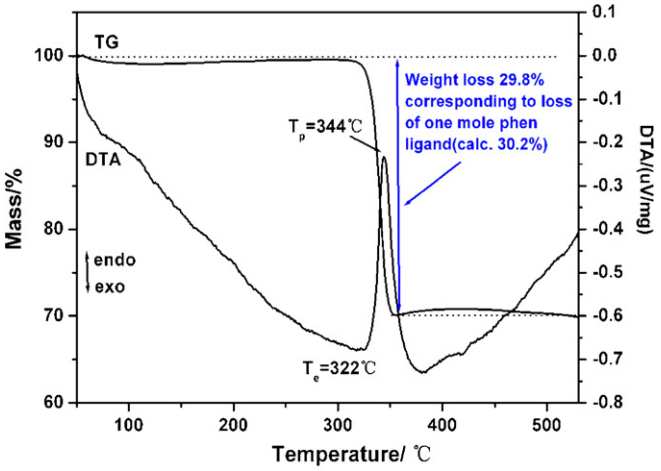

Fig. 5. TG–DTA curves of **1**.

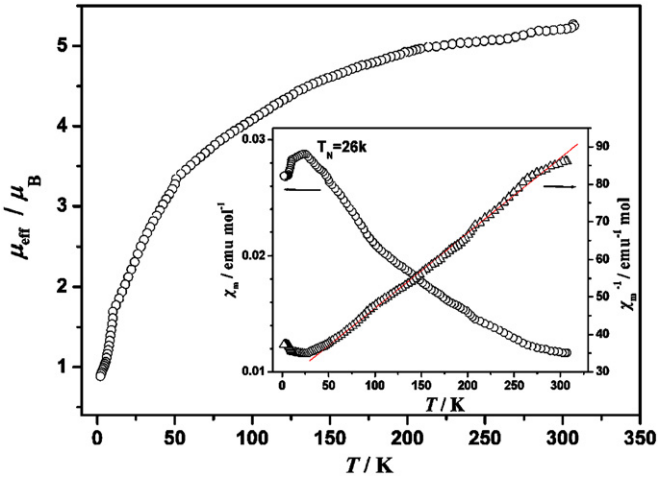

Fig. 7. The temperature dependencies of the effective magnetic moment for compound **1**. The inset shows magnetic susceptibility (χ_m, open rounds) and inverse magnetic susceptibility ($1/\chi_m$, open trigons) plotted as a function of temperature for **1**.

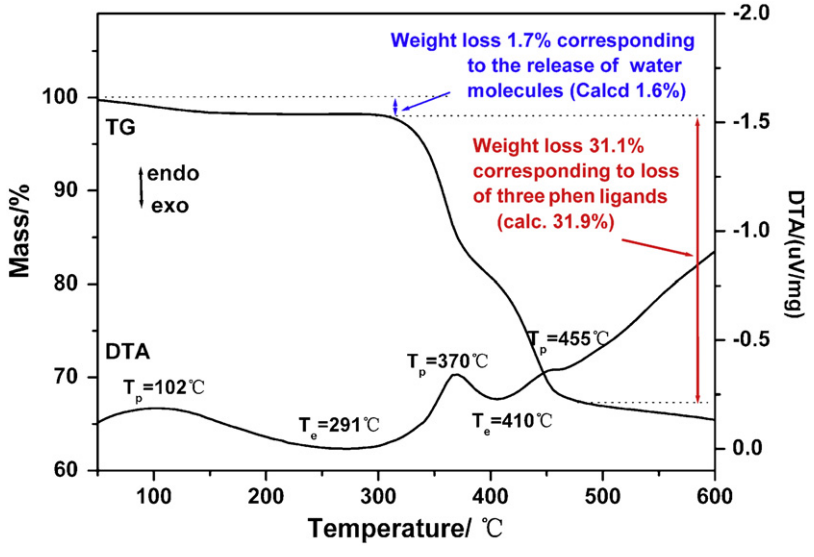

Fig. 6. TG–DTA curves of **2**.

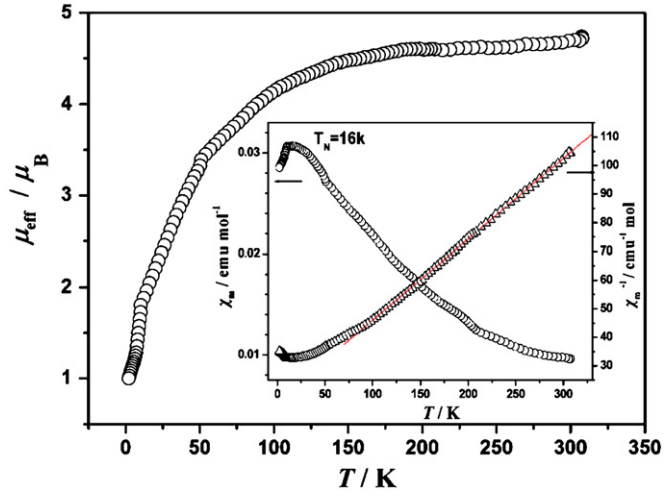

Fig. 8. The temperature dependencies of the effective magnetic moment for compound **2**. The inset shows magnetic susceptibility (χ_m, open rounds) and inverse magnetic susceptibility ($1/\chi_m$, open trigons) plotted as a function of temperature for **2**.

compounds. On the [100] plane of compound **1**, the 18-membered rings within the 2D porous layers of (6,3) topology are formed by corner-, edge-, and face-sharing of cubane-like $[Mn_2As_2S_4]$ units, which are constructed by trigonal pyramidal $[AsS_3]$ units, $[MnN_2S_4]$ and $[MnS_6]$ octahedra. In compound **2**, two $[MnN_2S_4]$ octahedra are edged-shared by two S atoms to form the $[Mn_2]$ unit, and then the $[Mn_2]$ units are edge-shared with two $[AsS_4]$ tetrahedra further. Finally the 1D neutral chain is formed through the connection of this $[Mn_2As_2]$ unit with another $[MnN_2S_4]$ octahedron fragment along [001] direction. Both of the two compounds are semiconductors, and the variable-temperature magnetic susceptibility data suggest weak antiferromagnetic interactions between Mn^{2+} ions in these two compounds.

Supporting information available

Crystallographic information files (CIF), IR spectra, Powder XRD patterns, The energy dispersive X-ray spectra.

Acknowledgments

This work was supported by Grants from the 973 Program (2007CB815301 and 2006CB932904), the National Science Foundation of China (20333070, 20673118, 20871114), the Science Foundation of CAS (KJCX2-YW-M05) and of Fujian Province (2006L2005, 2006J0014, 2006F3132).

Appendix A. Supplementary materials

Supplementary data associated with this article can be found in the online version at: doi:10.1016/j.jssc.2009.01.021.

References

[1] G.W. Drake, J.W. Kolis, Coord. Chem. Rev. 137 (1994) 131.
[2] C.L. Bowes, G.A. Ozin, Adv. Mater. 8 (1996) 13.
[3] W.S. Sheldrick, M. Wachhold, Angew. Chem. Int. Ed. 36 (1997) 206.
[4] J.H. Liao, G.M. Marking, K.F. Hsu, Y. Mastsushita, M.D. Ewbank, R. Borwick, P. Cunningham, M.J. Rosler, M.G. Kanatzidis, J. Am. Chem. Soc. 125 (2003) 9484.
[5] Z. Chen, R. Wang, J. Li, Chem. Mater. 12 (2000) 762.
[6] N.F. Zheng, X.H. Bu, B. Wang, P.Y. Feng, Science 298 (2002) 2366.
[7] M.E. Davis, Nature 417 (2002) 813.
[8] X.T. Wu, Q. Huang, Q.M. Wang, T.L. Sheng, J.X. Lu, In: Stiefel, E. I., Matsumoto, K. (Eds.), Transition Metal Sulfur Chemistry: Biological and Industrial Significance, ACS Symposium Series, Vol. 653, American Chemical Society, Washington, DC, 1996, p. 282.
[9] L. Chen, X.T. Wu, In: G. Meyer, D. Naumann, L. Weseman (Eds.), Inorganic Chemistry in Focus II, 2005, p. 207.
[10] X.T. Wu, P.C. Chen, S.W. Du, N.Y. Zhu, J.X. Lu, J. Clust. Sci. 5 (1994) 265.
[11] S.W. Du, N.Y. Zhu, P.C. Chen, X.T. Wu, Angew. Chem. Int. Ed. 31 (1992) 1085.
[12] H. Yu, W.J. Zhang, X.T. Wu, T.L. Sheng, Q.M. Wang, P. Lin, Angew. Chem., Int. Ed. 37 (1998) 2520.
[13] X. Wang, T.L. Sheng, R.B. Fu, S.M. Hu, S.C. Xiang, L.S. Wang, X.T. Wu, Inorg. Chem. 45 (2006) 5236.
[14] M. Zhang, T.L. Sheng, X.H. Huang, R.B. Fu, X. Wang, S.M. Hu, S.C. Xiang, X.T. Wu, Eur. J. Inorg. Chem. (2007) 1606.
[15] M. Wachhold, M.G. Kanatzidis, Inorg. Chem. 38 (1999) 3863.
[16] J.A. Hanko, J.-H. Chou, M.G. Kanatzidis, Inorg. Chem. 37 (1998) 1670.
[17] J.-H. Chou, M.G. Kanatzidis, Chem. Mater. 7 (1995) 5.
[18] J.-H. Chou, M.G. Kanatzidis, Inorg. Chem. 33 (1994) 1001.
[19] V. Vater, W.S. Sheldrick, Z. NAturforsch. B Chem. Sci. 52 (1997) 1119.
[20] M.L. Fu, G.C. Guo, X. Liu, B. Liu, L.Z. Cai, J.S. Huang, Inorg. Chem. Commun. 8 (2005) 18.
[21] D.X. Jia, Q.X. Zhao, J. Dai, Y. Zhang, Q.Y. Zhu, Z. Anorg. Allg. Chem. 632 (2006) 349.
[22] M.L. Fu, G.C. Guo, L.Z. Cai, Z.J. Zhang, J.S. Huang, Inorg. Chem. 44 (2005) 184.
[23] Y.L. An, X.F. Li, X. Liu, M. Ji, C.Y. Jia, Inorg. Chem. Commun. 6 (2003) 1137.
[24] M.L. Fu, G.C. Guo, X. Liu, W.T. Chen, B. Liu, J.S. Huang, Inorg. Chem. 45 (2006) 5793.
[25] Y.D. Wu, C. Näther, W. Bensch, Inorg. Chem. 45 (2006) 8835.
[26] Q.C. Zhang, X.H. Bu, Z.E. Lin, M. Biasini, W.P. Beyermann, P.Y. Feng, Inorg. Chem. 46 (2007) 7262.
[27] M.L. Fu, G.C. Guo, X. Liu, W.T. Chen, B. Liu, J.S. Huang, Inorg. Chem. 45 (2006) 5793.
[28] A. Kromm, W.S. Sheldrick, Z. Anorg. Allg. Chem. 634 (2008) 121.
[29] A. Kromm, W.S. Sheldrick, Z. Anorg. Allg. Chem. 634 (2008) 225.
[30] G.M. Sheldrick, SHELXS 97, Program for Crystal Structure Solution, University of Göttingen, Göttingen, 1997.
[31] G.M. Sheldrick, SHELXS 97, Program for Crystal Structure Refinement, University of Göttingen, Göttingen, 1997.
[32] D.X. Jia, Y. Zhang, J. Dai, Q.Y. Zhu, X.M. Gu, J. Solid State Chem. 177 (2004) 2477.
[33] D.X. Jia, Q.X. Zhao, J. Dai, Y. Zhang, Q.Y. Zhua, Z. Anorg. Allg. Chem. 632 (2006) 349.
[34] J.H. Chou, M.G. Kanatzidis, Chem. Mater. 7 (1995) 5.
[35] J.H. Chou, M.G. Kanatzidis, Inorg. Chem. 33 (1994) 5372.
[36] J.H. Chou, J.A. Hanko, M.G. Kanatzidis, Inorg. Chem. 36 (1997) 4.
[37] Z. Hu, L.Q. Dang, D.H. Bao, Y.L. An, Acta Cryst. E 62 (2006) m2756.
[38] M. Schur, W. Bensch, Z. Naturforsch. B Chem. Sci. 57 (2002) 1.
[39] A. Puls, C. Näther, W. Bensch, Z. Anorg. Allg. Chem. 632 (2006) 1239.
[40] J.-H. Chou, J.A. Hanko, M.G. Kanatzidis, Inorg. Chem. 36 (1997) 4.
[41] W.M. Wendlandt, H.G. Hecht, Reflectance Spectroscopy, Interscience, New York, 1966.